Optical Kerr Effect Spectroscopy of CS2 in Monocationic and Dicationic Ionic Liquids: Insights into the Intermolecular Interactions in Ionic Liquids

Journal:	*Physical Chemistry Chemical Physics*
Manuscript ID	CP-ART-07-2018-004503.R1
Article Type:	Paper
Date Submitted by the Author:	01-Oct-2018

Complete List of Authors:	Gurung, Eshan; Texas Tech University, Chemistry & Biochemistry Meng, Dujuan; Texas Tech University, Chemistry & Biochemistry Xue, Lianjie; Texas Tech University, Chemistry & Biochemistry Tamas, George; Texas Tech University, Chemistry & Biochemistry Lynden-Bell, Ruth; University of Cambridge, Department of Chemistry Quitevis, Edward; Texas Tech University, Chemistry and Biochemistry

Optical Kerr Effect Spectroscopy of CS_2 in Monocationic and Dicationic Ionic Liquids: Insights into the Intermolecular Interactions in Ionic Liquids

Eshan Gurung,[1] Dujuan Meng,[1] Lianjie Xue,[1#] George Tamas,[1#] Ruth M. Lynden-Bell,[2] Edward L. Quitevis[1]*

[1]Department of Chemistry & Biochemistry, Texas Tech University, Lubbock, TX 79409, USA

[2]Department of Chemistry, University of Cambridge, Lensfield Road, Cambridge, CB2 1EW, UK

[#]Current addresses:

L. Xue – Department of Physics, Kansas State University, Manhattan, KS 66506 USA

G. Tamas – YTC America Inc., Camarillo, CA 93012 USA

*To whom correspondences should be addressed:

edward.quitevis@ttu.edu

Abstract

A comparative study of the intermolecular dynamics of CS_2 in monocationic and dicationic ionic liquids (ILs) was performed using optical heterodyne-detected Raman-induced Kerr effect spectroscopy (OHD-RIKES). The reduced spectral densities (RSDs) of mixtures of CS_2 in 1-alkyl-3-methylimidazolium bis[(trifluoromethane)sulfonyl]amide ($[C_nC_1im][NTf_2]$ for n = 3-5) and 1,2n-bis(3-methylimidazolium-1-yl) alkane bis[(trifluoromethane)sulfonyl]amide ($[(C_1im)_2C_{2n}][NTf_2]_2$ for n = 3-5) were investigated as a function of concentration at 295 K. An

additivity model was used to obtain the CS_2 contribution to the RSD of a mixture in the 0-200 cm^{-1} region. One of the aims of this study is to show how CS_2 can be used as a probe of intermolecular/interionic interactions in ILs. The concentrations were chosen such that the CS_2-to-imidazolium ring mole fraction of a mixture with $[(C_1im)_2C_{2n}][NTf_2]_2$ (DIL(2*n*)) is the same as that of a mixture with $[C_nC_1im][NTf_2]$ (MIL(*n*)). As found previously for CS_2 in monocationic ILs the intermolecular spectrum of CS_2 in dicationic ILs is lower in frequency and narrower than that of neat CS_2. The new result is that the intermolecular spectrum of CS_2 is higher in frequency in DIL(2*n*) than in the corresponding MIL(*n*), indicating that CS_2 molecules experience a stiffer potential in dicationic ILs than in monocationic ILs. That the intermolecular dynamics of CS_2 are higher in frequency in DIL(2*n*) than in MIL(*n*) is consistent with recent molecular dynamics simulations (Lynden-Bell and Quitevis, *J. Chem. Phys.*, 2018, **148**, 193844) that show the stiffer potential is the result of greater confinement of CS_2 in DIL(2*n*) than in MIL(*n*). We also show in this study how effects due to dilution and the intermolecular potential seen by a solute molecule in solution are unraveled.

1. Introduction

Room-temperature ionic liquids (ILs) are defined as organic salts with melting points at or below 100°C.[1] ILs have been used as solvents in synthesis, electrochemistry, separations, engineering, and other applications.[1, 2] They are often referred to as "green designer" solvents due to their negligible vapor pressure, ease of recycling, and the ability to tune their properties through structural modifications of the cation and variation of the anion.[3-5]

ILs are different than conventional molecular solvents in two major aspects, the first obviously being that they are entirely composed of ions, which results in higher binding energies than found in polar and nonpolar liquids. As such, the tendency to maintain charge neutrality means that interactions between ions of the opposite charge are maximized, whereas interactions between ions of the same charge are minimized. This self-organizing behavior of ILs, often referred to as "charge ordering," results in charge alternation in the local structure. The second unique aspect of ILs is the existence of nano-segregation, which was first observed in molecular dynamics (MD) simulations of ILs based on 1-alkyl-3-methylimidazolium ($[C_nC_1im]^+$) cations.[6-8] This nano-segregation is characterized by the aggregation of alkyl chains of ILs to form nonpolar domains, which are embedded in the polar ionic network. The experimental evidence for nano-segregation in ILs is a low-Q peak (i.e., pre-peak) in the small-wide angle X-ray scattering (SWAXS) from ILs, such as ones based on the $[C_nC_1im]^+$ cation,[9-11] that shifts to lower Q-values with increasing chain length. The assignment of the pre-peak to nano-segregation in ILs is well supported by MD simulations of the X-ray structure factor function $S(Q)$.[12]

One of the consequences of nano-segregation in ILs, as shown by MD simulations of molecular-solute/IL mixtures, is that solute molecules experience different solvation environments depending on their polarity, aromaticity, and proticity.[13-15] Nonpolar solutes, such

as *n*-hexane, tend to be localized in the nonpolar domains, polar aprotic solutes, such as acetonitrile, at the interface between the polar domains and the ionic network, and polar protic solutes, such as methanol and water, in the ionic network.

Probing these different solvation environments experimentally has been a major focus of our research group and other research groups. Of particular interest is the solvation environment of the nonpolar nonaromatic solutes such as CS_2. Our approach has been to use optical heterodyne-detected Raman-induced Kerr effect spectroscopy (OHD-RIKES) to study the intermolecular dynamics of CS_2 in $[C_nC_1im][NTf_2]$ with $[NTf_2]^-$ being the bis[(trifluoromethane)sulfonyl]amide anion.[16-18] OHD-RIKES is a nonlinear optical time-domain method that measures a quantity related to the negative time-derivative of the total polarizability anisotropy time-correlation function (TCF) of a liquid.[19-21] OHD-RIKES has been extensively applied to the study of the low-frequency intermolecular vibrational modes of liquids,[19-23] and in recent years to that of ILs.[11, 16-18, 24-49] It is complementary to dielectric spectroscopy.[38] To glean information about the intermolecular dynamics, the part of the OHD-RIKES signal relaxing on ps-ns timescales associated with the reorientational dynamics is removed, generating a "reduced" response comprising only the electronic and the sub-picosecond nuclear responses. By use of a Fourier-transform-deconvolution procedure, the reduced response can be converted to a reduced spectral density (RSD) (i.e., OKE or Kerr spectrum).[50, 51] The RSD is directly related to the Bose-Einstein prefactor-weighted depolarized Rayleigh/Raman spectrum of the liquid.[52] In the case of CS_2/IL mixtures, the contribution of CS_2 to the RSD of the mixture is obtained by use of an additivity model.[17, 18]

Previous studies[16-18] in our labs showed that the intermolecular spectrum of CS_2 is lower in frequency in CS_2/IL mixtures than in neat CS_2. Based on the similarity of the spectra of CS_2 in

IL and alkane mixtures, we concluded that CS_2 molecules are primarily localized in the nonpolar domain, a conclusion also supported by MD simulations.[17, 53] We recently found that the spectrum of CS_2 is higher in frequency in $[C_1C_1im][NTf_2]$ than in $[C_4C_1im][NTf_2]$,[18] which MD simulations show to be due to CS_2 molecules localized near the hydrogen at the C2 position of imidazolium ring in $[C_1C_1im][NTf_2]$ versus being near the terminal methyl group on the butyl chain in $[C_4C_1im][NTf_2]$.[53] These results suggest that CS_2 might be a useful probe of the intermolecular interactions in other ILs. In this paper we explore the implications of this idea in a comparative study of the RSDs of mixtures of CS_2 in geminal dicationic ILs, 1,n-bis(3-methylimidazolium-1-yl) alkane bis[(trifluoromethane)sulfonyl]amide, $[(C_1im)_2C_{2n}][NTf_2]_2$ (n = 3-5) and of mixtures of CS_2 in monocationic ILs $[C_nC_1im][NTf_2]$ (n = 3-5) as a function of concentration at 295 K.

Dicationic ILs are thermally more stable, are in the liquid state over a wider temperature range, and have higher shear viscosities, surface tensions, and liquid densities than monocationic ILs with the same anion and comparable alkyl group.[54-56] Although the structural heterogeneity in monocationic ILs has been extensively studied, it has not been extensively studied in dicationic ILs. Bobo et al.[57] performed MD simulations on $[(C_1im)_2C_n][NTf_2]_2$ for n = 3, 6, 9, and 12. In these studies, the simulated X-ray structure factor $S(Q)$ of dicationic ILs was found to be similar to that of monocationic ILs, with a high-Q peak associated with direct contact cation-anion pairs and an intermediate-Q peak assigned to co-ion correlations associated with close-distance ions of the same sign within the charge alternation. However, only in the case of $[(C_1im)_2C_{12}][NTf_2]_2$ did the simulated X-ray structure factor show a low-Q peak associated with alkyl chain aggregation. Bobo et al. speculated that the decrease in the degree of nano-segregation is due to the alkyl chains being less free. Li et al.[58] performed more detailed MD

simulations on $[C_nC_1im][BF_4]$ with n = 3, 6, and 8, and $[(C_1im)_2C_n][BF_4]_2$ with n = 3, 6, 9, 12, and 16. As shown previously in the case of monocationic ILs, structural heterogeneity was observed with elongation of the alkyl chain in dicationic ILs. However, based on the heterogeneity order parameter, dicationic ILs have a lower degree of alkyl chain aggregation than monocationic ILs. Pre-peaks in the $S(Q)$s were observed for $[C_6C_1im][BF_4]$ and $[C_8C_1im][BF_4]$, but not for $[C_3C_1im][BF_4]$, and for $[(C_1im)_2C_{12}][BF_4]_2$ and $[(C_1im)_2C_{16}][BF_4]_2$, but not for $[(C_1im)_2C_6][BF_4]_2$. In the case of short-chain ILs, $[(C_1im)_2C_6][BF_4]_2$ and $[C_3C_1im][BF_4]$, the $S(Q)$s were almost identical. In the case of medium-chain length ILs, the pre-peak was noticeable for $[C_6C_1im][BF_4]$, whereas it was less pronounced for $[(C_1im)_2C_{12}][BF_4]_2$. In the case of long-chain length ILs, the pre-peak was more pronounced for $[C_8C_1im][BF_4]$ than for $[(C_1im)_2C_{16}][BF_4]_2$. Li et al. attributed the lower degree of alkyl chain aggregation to the alkyl linker being constrained by the imidazolium rings at two ends, resulting in decreased flexibility of the alkyl chain.

The objective of this study is to determine how the dynamics of CS_2 in dicationic ILs differs from that in monocationic ILs. Given the difference in the properties of dicationic ILs as compared to those of monocationic ILs as described above, we hypothesize that the intermolecular spectrum of CS_2 should be higher in frequency in $[(C_1im)_2C_{2n}][NTf_2]_2$ than in $[C_nC_1im][NTf_2]$, indicating that CS_2 molecules experience a stiffer potential in dicationic ILs than in monocationic ILs. Preliminary results of this study were reported in a paper focused primarily on MD simulations of CS_2 in the monocationic IL, $[C_4C_1im][NTf_2]$, and the dicationic IL, $[(C_1im)_2C_8][NTf_2]_2$.[59] These simulations showed that the stiffer potential is the result of greater confinement in the liquid.

2. Experimental

2.1 Synthesis of the ionic liquids

The monocationic ILs, $[C_nC_1im][NTf_2]$ (n = 3-5), were synthesized following the general procedure summarized below in Scheme 1, which is based on procedures published by Bartsch and coworkers,[60, 61] with modifications. The details of this procedure and the purification of the ILs are summarized in the Electronic Supplementary Information (ESI).

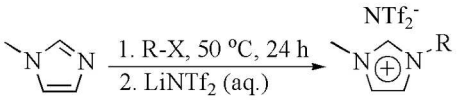

Scheme 1. Generic synthesis of $[C_nC_1im][NTf_2]$ with R = C_nH_{2n+1}.

The dicationic ILs, $[(C_1im)_2C_{2n}][NTf_2]_2$ (n = 3-5), were synthesized following the procedure summarized below in Scheme 2. The details of this procedure and the purification of the ILs are summarized in the ESI. For brevity, the monocationic ILs $[C_nC_1im][NTf_2]$ and dicationic ILs $[(C_1im)_2C_{2n}][NTf_2]_2$ will be referred to in this paper, respectively, as MIL(n) and DIL(2n).

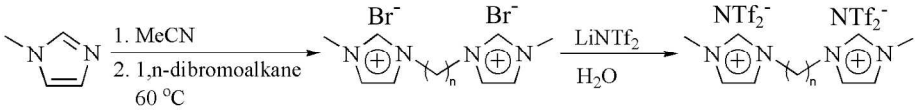

Scheme 2. Generic synthesis of $[(C_1im)_2C_{2n}][NTf_2]_2$ for n = 3-5.

2.2 Preparation of CS_2/IL Mixtures

The water contents of the ILs used in this study were < 100 μg/g, as determined by Karl-Fischer titration. CS_2 (Aldrich, spectrochemical grade) was used without further purification. 10, 15, 20, and 25 mol.% mixtures of CS_2 in MIL(n) for n = 3-5 and 18.2, 26, 33.3, and 40 mol. % mixtures of CS_2 in DIL(2n) for n = 3-5 were prepared in an argon-filled glove box. The samples were completely miscible and optically clear at the concentrations chosen for this study. The concentrations of the mixtures were chosen so that the mole fraction of imidazolium rings in a CS_2/DIL(2n) mixture is the same as that in a CS_2/MIL(n) mixture with the same n. (i.e., 10 mol. % CS_2/MIL(n) equivalent to 18.2 mol. % CS_2/DIL(2n), etc.). This choice of concentrations

allows us to see how the intermolecular dynamics of CS_2 are changed in going from the alkyl tails being free (i.e., CS_2/MIL(*n*) mixtures) to their tails being tied together (i.e., CS_2/DIL(2*n*) mixtures).

2.3 OHD-RIKES Apparatus and Procedures

Details of the OHD-RIKES apparatus have been presented previously.[24, 62, 63] We briefly describe herein the apparatus and data acquisition. A lab-built, self-mode-locked Titanium:sapphire laser, pumped by a Coherent Verdi V6 laser, produces a train of 38(3) fs pulses at a repetition rate of 82 MHz. A (0°/45°/-45°) polarization configuration is used for the pump, probe, and analyzer polarizers, with a λ/4-plate inserted in the probe beam before the sample.[64] Stray birefringence, such as from the windows of the sample cell, are nulled by adjusting the λ/4-plate. A local oscillator (LO) field, E_{LO}, for the signal field, E_S, is introduced by a slight misalignment (±δ°) of the probe polarizer.[64] The difference of the in-phase (+δ°) and out-of-phase (-δ°) signals gives the heterodyne contribution, $Re[E_{LO} \cdot E_S^*]$. A lab-built copper cell holder, whose temperature is regulated and controlled with a thermoelectric heater/cooler system, is used to control the temperature of the sample. For the current measurements the temperature was set at 295 K. A typical data set is the average of least 15 scans. To save time, scans were performed in 10-fs steps for time delays in the -1 to 4 ps range and in 50-fs steps in the 4 ps to 10 ps range. Shirota and Kakinuma[48] found that the time range of -1 to 10 ps is adequate for determining the RSDs of ILs. They showed that the RSDs from Kerr transients in the -1.5 to 8 ps time range and the -1.5 to 300 ps time range were the same intensity-wise within 1-2%. Representative OHD-RIKES time-domain data, fits of an empirical decay function to the data, and a brief description of the Fourier-transform-deconvolution procedure for obtaining the RSDs are given in the ESI.

3. Results and Analysis

3.1 Reduced spectral densities

The RSDs of neat CS_2, the neat ILs, and the CS_2/IL mixtures in the 0-400 cm^{-1} region are shown in Figure 1. The RSDs exhibit spectral features that are characteristic of typical $[NTf_2]^-$-based imidazolium ILs.[11, 24-26, 33, 42, 43, 45] These features include a broad, structured main band in the 0-200 cm^{-1} region associated with intermolecular/interionic vibrational modes, a low-intensity, high-frequency tail, and peaks in the 280-350 cm^{-1} region and at 407 cm^{-1} associated mainly with intramolecular vibrational modes of $[NTf_2]^-$. In contrast, the RSD of neat CS_2 in this frequency region is a single intermolecular band that is lower in frequency (peak frequency ω_{pk} = 28 cm^{-1}) and narrower (full-width at half maximum $\Delta\omega$ = 60 cm^{-1}) than that of the ILs.

The broad main band in the 0-200 cm^{-1} region of the RSDs of the neat ILs is characterized by a narrow low-frequency feature at ≈ 20 cm^{-1} associated with the intermolecular vibrations of the $[NTf_2]^-$ anion and/or cation translational-rotational vibrations, as shown by Shirota and coworkers,[39, 42] and a broad high-frequency feature at ≈ 70 cm^{-1} associated with the intermolecular vibrations of the cation. Superimposed on the intermolecular band is a small peak at ≈ 120 cm^{-1} associated with an intramolecular mode of the anion. The overlapping broad peaks at ≈ 170 and ≈ 210 cm^{-1} that contribute to the high-frequency tail are assigned to the intramolecular vibrations of the cation.[43]

The RSDs of the neat ILs shown in Figure 1 are consistent with those obtained previously by Shirota and Ishida.[43, 65] In particular, the pattern in the intensity of the high-frequency component band at ≈ 70 cm^{-1} relative to that of low-frequency component band at ≈ 20 cm^{-1} is similar to what was observed by Shirota and Ishida. This pattern can be best seen in Figure 2 where the RSDs of a MIL(n)/DIL(2n) pair with a given n have been normalized at the peak of

the low-frequency component band and plotted together. From these plots we see that the ratio I_{Hi}/I_{Lo}, corresponding to ratio of the intensity of the high-frequency component band to that of the low-frequency component, is < 1 for MIL(3), whereas it is > 1 for DIL(6). In contrast, the ratio I_{Hi}/I_{Lo} is nearly the same for both MIL(4) and DIL(8) and ≈ 1, and similarly for both MIL(5) and DIL(10).

In principle, the RSD of a liquid depends on the square of the derivative of the polarizability anisotropy $(\partial\Pi_{anis}/\partial q)^2$, where q is a canonical coordinate associated with one of the modes of a liquid.[66] Based on a comparison of the polarizability derivatives of the $[NTf_2]^-$ anion, the alkyl chain, and the imidazolium ring, Giraud et al.[25] estimated that the largest contribution to the RSDs of imidazolium-based ILs comes from the motion of the imidazolium rings and the smallest from the motion of the alkyl chains. That the largest contribution comes from the imidazolium ring is supported by OKE measurements of MIL(n)s that indicate the RSDs for $n \geq 3$ are not strongly dependent on alkyl chain length.[11] Therefore, as suggested by Shirota and Ishida,[43] the pattern exhibited by the relative intensities of the low- and high-frequency components of the intermolecular bands in MILs and DILs is reflection of the environment within the ionic networks. Specifically, the ratio I_{Hi}/I_{Lo} being nearly the same for both MIL(4) and DIL(8), and the same for both MIL(5) and DIL(10), means that the local structures in the ionic networks are the same for these ILs, whereas the ratio I_{Hi}/I_{Lo} being different for MIL(3) and DIL(6) means that the local structures in the ionic networks are different for these two ILs. To understand further the difference in the RSDs of MIL(3) and DIL(6), Ishida and Shirota[65] performed a comparative study of the dynamical properties of these two ILs using MD simulations. They ascribed the distinctive RSDs of MIL(3) and DIL(3) to differences in the angular momenta about specific body-fixed axes of $[C_3C_1im]^+$ as compared that of $[(C_1im)_2C_6]^+$

and differences in the relaxation behavior as determined by the mean-squared displacement of the centers of mass of the monocation and dication and by the second non-Gaussian parameter $\alpha_2(t)$.

3.2 Reduced spectral densities of CS_2/IL mixtures

In contrast to the neat ILs, the intermolecular part of the RSDs of CS_2/IL mixtures in the 0-120 cm^{-1} region is narrower and lower in frequency than that of the RSDs of the neat ILs (Figure 1). These differences are due to the RSD of a mixture arising not only from the intermolecular modes of the IL but also from the intermolecular modes of CS_2, which are lower in frequency than that of the IL. That the RSDs of the CS_2/IL mixtures and the neat ILs are well overlapped in the 120-250 cm^{-1} region and in the 250-400 cm^{-1} region indicates that CS_2 does not strongly affect the intramolecular modes of $[NTf_2]^-$.

3.3 Analysis of the mixture RSDs

The total polarizability anisotropy TCF of a CS_2/IL mixture will have contributions from CS_2 and the IL. The total polarizability anisotropy TCF of a mixture can therefore be partitioned into two autocorrelations corresponding to the collective polarizability anisotropy of CS_2 and the IL and a cross-correlation involving the collective polarizabilities anisotropies of both CS_2 and the IL. This results in the RSD of the mixture being given by

$$I_{mix}(\omega) = I_{CS_2}(\omega) + I_{IL}(\omega) + I_{CS_2-IL}(\omega) \quad (1)$$

where $I_{CS_2}(\omega)$ and $I_{IL}(\omega)$ are associated with the vibrational modes of CS_2 and the IL, respectively, and $I_{CS_2-IL}(\omega)$ is a cross-term associated with coupling of the vibrational modes of the two components. Cation-anion and tail-tail radial distribution functions (RDFs) obtained from MD simulations of 5, 10, and 20 mol % CS_2/$[C_5C_1im][NTf_2]$ mixtures[17] show that the structure of the IL is not strongly affected by the presence of CS_2 in the IL. The IL term in eq 1

can thus be approximated by the RSD of the neat IL. Secondly, based on the MD-simulation RDFs between CS_2 and the various groups of the IL, there is a higher probability of CS_2 molecules of being near terminal groups of the alkyl chains than near the head-groups or anions in the polar network.[17] Given that the polarizability of the IL being mainly determined by the groups in the ionic network, we can therefore conclude that the cross term in eq 1 should be smaller than the other two terms in eq 1. If these conditions hold for CS_2/IL mixtures, eq 1 reduces to an additivity model expression

$$I_{mix}(\omega) \approx I_{CS_2}(\omega) + \lambda_{IL} I_{IL}^{neat}(\omega) \quad (2)$$

where $I_{IL}^{neat}(\omega)$ is the RSD of the neat IL and λ_{IL} is a weight factor that accounts for relative contributions of CS_2 and the IL to the mixture RSD.

Using eq 2 to analyze the spectra of CS_2/IL mixtures neglects the $I_{CS_2-IL}(\omega)$ cross term. This dilemma can be resolved by folding the $I_{CS_2-IL}(\omega)$ cross-term into an effective CS_2 term $I_{CS_2}^{eff}(\omega)$ that results in the mixture spectrum being given by

$$I_{mix}(\omega) \approx I_{CS_2}^{eff}(\omega) + \lambda_{IL} I_{IL}^{neat}(\omega) \quad (3)$$

with

$$I_{CS_2}^{eff}(\omega) \equiv I_{CS_2}(\omega) + I_{CS_2-IL}(\omega) \quad (4)$$

Mathematically, the additivity model in eq 3 is identical to the additivity model in eq 2. The only difference is in the way in which $I_{CS_2}^{eff}(\omega)$ is interpreted as arising from intermolecular vibrations associated with the collective motions of CS_2 molecules and intermolecular vibrations associated with the correlated motions of CS_2 molecules with various groups in the IL.

To facilitate the fitting of the mixture RSDs by the additivity model, $I_{CS_2}^{eff}(\omega)$ can be

represented, as frequently done for other simple molecular liquids,[20] by a two-component line-shape function

$$I_{CS_2}^{eff}(\omega) = I_{BL}(\omega) + I_{AG}(\omega) \quad (5)$$

where the first term on the righthand side of the equation is the Bucaro-Litovitz (BL) function[67]

$$I_{BL}(\omega) = A_{BL}\omega^{\alpha}\exp(-\omega/\omega_{BL}) \quad (6)$$

and the second term is the anti-symmetrized Gaussian function

$$I_{AG}(\omega) = A_{AG}(\exp[-(\omega-\omega_{AG})^2/2\epsilon^2)] - \exp[-(\omega+\omega_{AG})^2/2\epsilon^2)]) \quad (7)$$

which is commonly assigned to librational modes that underlie the high-frequency side of the intermolecular band.[66] Fits of two-component line-shape function to the CS_2 contribution to the mixtures RSDs were performed by placing a physically motivated constraint on the amplitude of the AG function.[68] Because fits of the AG function are not well determined, the constrained results in more intuitive trends in the fits of the RSDs. Free fits yield values of ω_{AG} that are unrealistically too low, whereas constrained fits yield values of ω_{AG} that are consistent with the peak positions of the AG function.[68]

As can be seen in Figure 3, the RSD of neat CS_2 is well described by the two-component line-shape function with the low-frequency component being described by the Bucaro-Litovitz function and the high-frequency component by the antisymmerized Gaussian function. In Figure 4 are shown representative fits of the additivity model (eq 3) to the RSDs for 10 mol.% CS_2/MIL and 18.2 mol.% CS_2/DIL mixtures. Also shown in this figure are fits of the two-component line-shape function to the CS_2 contribution. Parameters for fits of the two-component line-shape function for the 10 mol.% CS_2/MIL and 18.2 mol.% CS_2/DIL mixtures are listed Table 1 and for the other CS_2/MIL and CS_2/DIL mixtures in Tables S2a-c in the ESI.

The height-normalized CS_2 contributions in each of the mixtures obtained from the fits of

the additivity model are compared with the RSD of neat CS_2 in Figure 5. For both mixture systems, $I_{CS_2}^{eff}(\omega)$ is narrower and lower in frequency than the RSD of neat CS_2. In Table 2 values of the peak frequency, ω_{pk}, and the full-width-at-half maximum, $\Delta\omega$, for CS_2 in 10, 15, 25 mol.% CS_2/MIL mixtures are compared to the corresponding values for CS_2 in 18.2, 26, 33.3, and 40 mol.% CS_2/DIL mixtures. It can be seen in Table 2 that for a given *n*, the intermolecular spectrum of CS_2 in DILs is higher in frequency than in MILs, with the average peak frequency, $<\omega_{pk}>$ being 25(1) cm^{-1} in DIL(6) versus 22(2) cm^{-1} in MIL(3); 27(2) cm^{-1} in DIL(8) versus 22(2) cm^{-1} in MIL(4); and 25(2) cm^{-1} in DIL(10) versus 24(1) cm^{-1} in MIL(5).

In contrast to the values of ω_{pk}, the values of $\Delta\omega$ for CS_2 in the mixtures do not show a clear trend, with the average value being equal to 52 ± 2 cm^{-1} (95 percent, N = 24). One can however take into account the width of the band in characterizing the frequency of an intermolecular band $I(\omega)$ through the use of the spectral first moment

$$M_1 \equiv \int_0^{\omega_{max}} \omega I(\omega) d\omega \,/\, \int_0^{\omega_{max}} I(\omega) d\omega \qquad (8)$$

where the integration is over the band with ω_{max} (= 200 cm^{-1} in the case of CS_2) being low enough to exclude intramolecular vibrations. This quantity gives the average frequency of the band and therefore allows one to account for band asymmetry. Table 3 list the values of M_1 for CS_2 in CS_2/MIL(4) and CS_2/DIL(8) mixtures and in the neat CS_2. Clearly, because the spectrum of CS_2 is asymmetric, M_1 is greater than ω_{pk}. Interestingly, the difference in the values of M_1 and ω_{pk}, which is a measure of band asymmetry, is greater for CS_2 in CS_2/MIL(4) mixtures (average difference = 15(2) cm^{-1}) than in CS_2/DIL(8) mixtures (average difference = 11(1) cm^{-1}). If we assume heterogeneous broadening, the higher asymmetry implies higher local disorder for CS_2 in MILs than in DILs, which is consistent with the alkyl chains being freer in MILs than in DILs.

4. Discussion

4.1 Intermolecular dynamics of CS_2 in CS_2/IL mixtures versus in neat CS_2

As can be seen from Table 2 and Figure 5, the intermolecular spectrum of CS_2 in an IL, regardless of whether the IL is a MIL or a DIL, is lower in frequency and narrower than in neat CS_2. In an initial OHD-RIKES study of mixtures of CS_2 and $[C_5C_1im][NTf_2]$,[16] we had proposed the intermolecular spectrum of CS_2 in ILs being lower in frequency and narrower than that of the CS_2 in the neat liquid is due to CS_2 molecules being isolated from each other and localized in the nonpolar domains of the IL. The justification for this explanation is based on the CS_2 contribution to the RSD of a 5 mol.% $CS_2/C_5C_1im][NTf_2]$ mixture resembling that of a 5 mol.% CS_2/n-pentane mixture, with the spectrum being lower in frequency and narrower than that of neat CS_2. MD simulations of this mixture system showed that CS_2 are isolated from each other and mainly localized in the nonpolar domains.[17] A shift to lower frequency and narrowing of the spectrum are commonly observed in RSDs upon dilution in weakly interacting systems, such as CS_2 in alkane mixtures.[69-73]

The mechanism for these effects is however controversial.[72] In one mechanism the spectral changes arise from softening of the effective intermolecular potential seen by CS_2 molecules upon dilution.[74, 75] In another mechanism the spectral changes arise from a decrease in interaction-induced effects upon dilution.[72] In previous studies of CS_2/IL mixtures,[16-18, 76] we attributed the spectral changes primarily to softening of the intermolecular potential. However, based on MD simulations comparing the intermolecular dynamics of CS_2 in $[C_1C_1im][NTf_2]$ to that of CS_2 in $[C_4C_1im][NTf_2]$, Lynden-Bell and Quitevis[53] concluded that a decrease in interaction-induced (I-I) effects might also be contributing to the observed spectral changes for CS_2/IL mixtures.

For liquids comprised of anisotropic molecules, the collective polarizability anisotropy TCF

can be resolved into a molecular autocorrelation, an I-I autocorrelation, and a molecular-induced cross correlation.[77-79] Relaxation of the molecular term occurs through single-molecule rotation, whereas relaxation of the induced terms (autocorrelation and cross correlation) occurs through intermolecular motions. When reorientation and intermolecular motions are on the same timescales, which is the case for CS_2,[78, 79] the induced part of the polarizability that follows reorientation can be projected out. The TCF can then be written as the sum of a local-field modified molecular reorientation term, a collision-induced (CI) term, and a collision-induced cross correlation, with the CI terms contributing to the high-frequency part of the spectrum. Without invoking softening of the intermolecular potential, the red-shift and line-narrowing of the RSDs can therefore be explained by a decrease in the contribution of the high-frequency CI terms upon dilution in going from CS_2 molecules in the neat liquid to CS_2 molecules being isolated from each other in CS_2/IL mixtures. Interestingly, the low-frequency librational and translational densities of states for CS_2 calculated from MD simulations are lower in frequency in neat CS_2 than in either CS_2/[C_1C_1im][NTf_2] or CS_2/[C_4C_1im][NTf_2] mixtures. The density of states, being a single-molecule property, cannot account for collision-induced effects. The MD simulations also showed that the interaction energy is greater for CS_2 in ILs than in the neat CS_2. This would explain why the density of states is higher in frequency for CS_2 in ILs than in neat CS_2. If we assume that the molecular reorientation part of the polarizability anisotropy TCF behaves in the same way as the density of state, then the red-shift and line-narrowing of the RSD of CS_2 in going from the neat liquid to the mixtures cannot be due to softening of the intermolecular potential seen by the CS_2 but rather to a dilution effect that diminishes the role of the CI terms in the polarizability anisotropy TCF.

4.2 Intermolecular dynamics of CS_2 in dicationic ILs versus in monocationic ILs

It is clear from Tables 2 and 3 and Figure 6 that the CS_2 contribution is higher frequency in CS_2/DIL(2*n*) mixtures than in CS_2/MIL(*n*) mixtures with the same *n*. This difference suggests that CS_2 molecules experience a stiffer intermolecular potential in dicationic mixtures than in monocationic mixtures. In general, one expects the intermolecular potentials to be stiffer in the liquid with the higher density and/or viscosity.[20]

Table 4 shows a comparison of the densities and viscosities of the 10 mol.% CS_2/MIL(*n*) mixtures to that of the equivalent 18.2 mol.% CS_2/DIL(2*n*) mixtures. The densities of the mixtures were calculated using the densities and viscosities of the neat liquids and assuming additivity of molar volumes and fluidities.[‡] Whereas for a given *n*, the density of a CS_2/DIL(2*n*) mixture is 4% greater than that of the corresponding CS_2/MIL(*n*) mixture and the viscosity of a CS_2/DIL(2*n*) mixture twice that of the corresponding CS_2/MIL(*n*) mixture. That the intermolecular spectrum of CS_2 is higher in CS_2/DIL(2*n*) mixtures than in CS_2/MIL(*n*) mixtures is therefore consistent with the density and viscosity being higher in CS_2/DIL(2*n*) mixtures than in CS_2/MIL(*n*) mixtures.

It is also noteworthy that the values of ω_{AG} (see Table S3 in the ESI) are higher for CS_2 in DILs than in MILs with the average, $\langle\omega_{AG}\rangle$, being 36.2(6) cm^{-1} in DIL(6) versus 32.5(6) cm^{-1} in MIL(3); 36.0(6) cm^{-1} in DIL(8) versus 32.0(2) cm^{-1} in MIL(4); and 36.4(5) cm^{-1} in DIL(10) versus 31.9(2) cm^{-1} in MIL(5). This pattern in the values of $\langle\omega_{AG}\rangle$ parallels the pattern in the values of $\langle\omega_{pk}\rangle$. As stated above, the high-frequency component of the two-component model is commonly associated with the librational modes of a liquid.

4.3 MD Simulations

To understand further the results of this OHD-RIKES study, we draw upon recent MD NVT simulations performed on a system of 108 anions, 108/56 cations, and 12 CS_2 molecules

corresponding to 10 mol.% CS_2/MIL(4) and 18.2 mol.% CS_2/DIL(8) mixtures.[59] Figure 7 shows a comparison of the intermolecular spectra of CS_2 from OHD-RIKES measurements to the librational densities of state of CS_2 from these simulations. RSDs, which arise from fluctuations in the collective anisotropy, cannot in principle be compared to densities of states, which are calculated from single particle velocity correlation functions.[80] However, as explained above, dilution minimizes the role of the CI terms in the polarizability anisotropy TCF. For CS_2/IL mixtures, the RSDs are therefore primarily determined by the molecular autocorrelation, which relaxes through single-molecule rotation.

Although the maxima (ω_{pk} = 21 and 30 cm^{-1} for CS_2 in MIL(4) and DIL(8), respectively) and first spectral moments (M_1 = 35 and 40 cm^{-1} for CS_2 in MIL(4) and DIL(8), respectively) of the RSDs are different from those of the maxima (ω_{pk} = 29 and 34 cm^{-1} for CS_2 in MIL(4) and DIL(8), respectively) and first spectral moments (M_1 = 44 and 47 cm^{-1} for CS_2 in MIL(4) and DIL(8), respectively) of the densities of states, the shift to higher frequency observed in the OHD-RIKES measurements is qualitatively mirrored in the MD simulations. It should be noted that polarizability was not included in the MD force field.

To gain insight into the mechanism of the shift to higher frequency, M_1 for the translational and librational densities of states of CS_2 in the 18.2 mol.% CS_2/DIL(8) mixture were calculated as a function of pressure (or equivalently, ring/anion number density) by changing the size of the simulation box (Table I and Figure 4 in ref 59). The calculations showed that when the linker chains in the dications are cut, the pressure increases, causing M_1 to increase. This result is physically reasonable because cutting the linker chain in the dication while keeping the volume the same should result in the local environment of CS_2 becoming more crowded and entangled. However, when the liquid is allowed to expand to equalize the pressure, M_1 decreases until it is

lower than in the monocationic mixture.

RDFs between the central carbon site in CS_2 and the unique carbon (C_2) on the imidazolium ring provide a molecular-level understanding of the effect of density on these systems. The RDFs show increased probability of finding CS_2 molecules near the imidazolium rings in going from dicationic mixture at low pressure to monocationic mixture to the dicationic mixture at ambient conditions (Figure 5a in ref 59). A similar but less pronounced trend is found for the RDFs between CS_2 and the central nitrogen site on the $[NTf_2]^-$ anion (Figure 5b in ref 59). These trends are consistent with greater confinement. Interestingly, RDFs between CS_2 and carbon sites along the alkyl chains show a higher probability of finding CS_2 near the terminal methyl group of the C_4 chain of the monocation (Figure 6a in ref 59) than near any of the sites along the linker chain of dication (Figure 6b in ref 59).

The greater confinement in dicationic mixtures than in the monocationic mixtures is also reflected in the interaction energies of CS_2 molecules with their local environment (Table II in ref 59). At ambient pressure and 300 K, the average Lennard-Jones and Coulomb contributions to CS_2-IL interaction energy increases by ≈ 8-9% in going from MIL(4) to DIL(8), which is consistent with the increase in the frequencies of translational and librational densities of states.

5. Conclusions

That dicationic ILs are thermally more stable and have higher shear viscosities, surface tensions, and liquid densities than monocationic ILs with the same anion and comparable alkyl groups is not surprising. However, in contrast to divalent inorganic salts where the charges are localized on a single site, the positive charges are located on separate imidazolium rings that are tethered to each other by an alkyl chain. Having imidazolium rings at opposite ends of the alkyl chain however decreases the flexibility of the chain, resulting in greater confinement.

We showed that by measuring the RSDs of mixtures of CS_2 in MIL(n) and DIL(2n) for n = 3-5, CS_2 molecules see a stiffer intermolecular potential in DIL(2n) than in the corresponding MIL(n). The concentrations of the mixtures are such that the imidazolium ring concentration in a CS_2/MIL(n) mixture is equal to the ring concentration in a CS_2/DIL(2n) mixture with the same n. Application of the additivity model to the RSDs of the mixtures allowed us to separate the CS_2 contributions from the RSDs of the mixtures. As found in previous studies of CS_2 in MILs,[16-18, 76] the intermolecular spectra of CS_2 in the DILs are lower in frequency and narrower than that of neat CS_2. MD simulations of CS_2/MIL mixtures[53] indicate that the red shift and line narrowing are not due to CS_2 molecules seeing a softer intermolecular potential by being localized in the nonpolar domains, as initially proposed, but primarily due to a dilution effect.

In the current study we find that the intermolecular spectrum of CS_2 is higher in frequency in a CS_2/DIL(2n) mixture than in a CS_2/MIL(n) mixture, not because of greater electrostatic interaction in DILs than in MILs. In fact, for the simulation box representing 10 mol.% CS_2/MIL(4) and 18.2 mol.% CS_2/DIL(8) mixtures at the same anion number density and 300 K the total electrostatic energies are essentially the same for the monocationic and dicationic mixtures.[59] The shift to higher frequency occurs because of increased confinement in dicationic solution than in the monocationic mixtures. This explanation is supported by the MD simulations that show the librational and translational densities of states of CS_2 to be higher in frequency in the 18.2 mol.% CS_2/DIL(8) mixture than in the 10 mol.% CS_2/MIL(4) mixture at ambient conditions. The dependence of M_1 of the simulated CS_2 density of states on pressure and the CS_2-cation/anion RDFs provides further evidence for this confinement effect.

Electronic supplementary information available: Procedures for synthesis of the ILs; NMR data, representative OHD-RIKES signals in 0-4 ps and 0-10 ps ranges for CS_2 in MIL(3)

and DIL(6); parameters for fit of the empirical decay function to the OHD-RIKES signals; and fits parameters of the two-component line-shape function describing the RSDs of neat CS_2 and the CS_2 contribution to mixture RSDs.

Acknowledgements.

This research was supported by the National Science Foundation under grant CHE-1153077 to ELQ. We thank Dr. Vidura Thalangamaarchchige for help in synthesizing one of the ionic liquids.

Conflicts of interest.

There are no conflicts to declare.

Notes and References

‡The high volatility of CS_2 prevented us from accurately measuring the density and viscosity of these mixtures. That CS_2 tends to be localized in the nonpolar domains makes the additivity assumption more plausible.

1. N. V. Plechkova and K. R. Seddon, *Chem. Soc. Rev.*, 2008, **37**, 123-150.
2. P. Wasserscheid and T. Welton, eds., *Ionic Liquids in Synthesis*, Wiley-VCH, Weinham, Germany, 2008.
3. M. Freemantle, *Chem. Eng. News*, 1998, **76**, 32-37.
4. M. J. Earle, J. M. S. S. Esperanca, M. A. Gilea, J. N. A. Canongia Lopes, L. P. N. Rebelo, J. W. Magee, K. R. Seddon and J. A. Widegren, *Nature*, 2006, **439**, 831-834.
5. N. V. Plechkova and K. R. Seddon, in *Methods and Reagents for Green Chemistry: An Introduction*, eds. P. Tundo, A. Perosa and F. Zecchini, John Wiley & Sons, Inc., New York, 2007, pp. 105-130.
6. S. M. Urahata and M. C. C. Ribeiro, *J. Chem. Phys.*, 2004, **120**, 1855-1863.
7. Y. Wang and G. A. Voth, *J. Am. Chem. Soc.*, 2005, **127**, 12192-12193.

8. J. N. A. Canongia Lopes and A. A. H. Padua, *J. Phys. Chem. B*, 2006, **110**, 3330-3335.

9. A. Triolo, O. Russina, H.-J. Bleif and E. Di Cola, *J. Phys. Chem. B*, 2007, **111**, 4641-4644.

10. A. Triolo, O. Russina, B. Fazio, R. Triolo and E. Di Cola, *Chem. Phys. Lett.*, 2008, **457**, 362-365.

11. O. Russina, A. Triolo, D. Xiao, L. G. Hines, Jr., R. A. Bartsch, E. L. Quitevis, L. Gontrani, R. Caminiti, N. V. Plechkova and K. R. Seddon, *Journal of Physics-Condensed Matter*, 2009, **21**, 424121(1)-414121(9).

12. H. K. Kashyap, J. J. Hettige, H. V. R. Annapureddy and C. J. Margulis, *Chem. Commun.*, 2012, **48**, 5103-5105.

13. C. G. Hanke, N. A. Atamas and R. M. Lynden-Bell, *Green Chem.*, 2002, **4**, 107-111.

14. J. N. A. Canongia Lopes, M. F. Costa Gomes and A. A. H. Padua, *J. Phys. Chem. B*, 2006, **110**, 16816-16818.

15. A. A. H. Padua, M. F. Costa Gomes and J. N. A. Canongia Lopes, *Acc. Chem. Res.*, 2007, **40**, 1087-1096.

16. D. Xiao, L. G. Hines, Jr., R. A. Bartsch and E. L. Quitevis, *J. Phys. Chem. B*, 2009, **113**, 4544-4548.

17. P. Yang, G. A. Voth, D. Xiao, L. G. Hines Jr., R. A. Bartsch and E. L. Quitevis, *J. Chem. Phys.*, 2011, **135**, 034502(1)-034502(12).

18. L. Xue, G. Tamas, E. Gurung and E. L. Quitevis, *J. Chem. Phys.*, 2014, **140**, 164512(1)-164512(11).

19. S. Kinoshita, Y. Kai, T. Ariyoshi and Y. Shimada, *Int. J. Mod. Phys. B*, 1996, **10**, 1229-1272.

20. J. T. Fourkas, in *Ultrafast Infrared and Raman Spectroscopy*, ed. M. D. Fayer, Marcel Dekker, Inc., New York, 2001, pp. 473-512.

21. N. Smith and S. R. Meech, *Int. Rev. Phys. Chem.*, 2002, **21**, 75-100.

22. E. W. Castner, Jr. and M. Maroncelli, *J. Mol. Liquids*, 1998, **77**, 1-36.

23. H. Shirota, T. Fujisawa, H. Fukazawa and K. Nishikawa, *Bull. Chem. Soc. Jpn.*, 2009, **82**, 1347-1366.

24. B. R. Hyun, S. V. Dzyuba, R. A. Bartsch and E. L. Quitevis, *J. Phys. Chem. A*, 2002, **106**, 7579-7585.

25. G. Giraud, C. M. Gordon, I. R. Dunkin and K. Wynne, *J. Chem. Phys.*, 2003, **119**, 464-477.

26. J. R. Rajian, S. Li, R. A. Bartsch and E. L. Quitevis, *Chem. Phys. Lett.*, 2004, **393**, 372-377.

27. H. Shirota, A. M. Funston, J. F. Wishart and E. W. Castner, Jr., *J. Chem. Phys.*, 2005, **122**, 184512(1)-18512(12).

28. H. Shirota and E. W. Castner, Jr., *J. Phys. Chem. A*, 2005, **109**, 9388-9392.

29. H. Shirota and E. W. Castner, Jr., *J. Phys. Chem. B*, 2005, **109**, 21576-21585.

30. D. Xiao, J. R. Rajian, S. Li, R. A. Bartsch and E. L. Quitevis, *J. Phys. Chem. B*, 2006, **110**, 16174-16178.

31. D. Xiao, J. R. Rajian, A. Cady, S. Li, R. A. Bartsch and E. L. Quitevis, *J. Phys. Chem. B*, 2007, **111**, 4669-4677.

32. H. Shirota, J. F. Wishart and E. W. Castner, Jr., *J. Phys. Chem. B*, 2007, **111**, 4819-4829.

33. E. W. Castner, Jr., J. F. Wishart and H. Shirota, *Acc. Chem. Res.*, 2007, **40**, 1217-1227.

34. D. Xiao, J. R. Rajian, L. G. Hines, Jr., S. Li, R. A. Bartsch and E. L. Quitevis, *J. Phys. Chem. B*, 2008, **112**, 13316-13325.

35. D. Xiao, L. G. Hines, Jr., S. Li, R. A. Bartsch, E. L. Quitevis, O. Russina and A. Triolo, *J. Phys. Chem. B*, 2009, **113**, 6426-6433.

36. H. Shirota, K. Nishikawa and T. Ishida, *J. Phys. Chem. B*, 2009, **113**, 9831-9839.

37. H. Shirota, T. Fujisawa, H. Fukazawa and K. Nishikawa, *Bull. Chem. Soc. Jpn.*, 2009, **82**, 1347-1366.

38. D. A. Turton, J. Hunger, A. Stoppa, G. Hefter, A. Thoman, M. Walther, R. Buchner and K. Wynne, *J. Am. Chem. Soc.*, 2009, **131**, 11140-11146.

39. T. Fujisawa, K. Nishikawa and H. Shirota, *J. Chem. Phys.*, 2009, **131**, 244519(1)-24519(14).

40. D. Xiao, L. G. Hines Jr., M. W. Holtz, K. Song , R. A. Bartsch and E. L. Quitevis, *Chem. Phys. Lett.*, 2010, **497**, 37-42.

41. H. Shirota, H. Fukazawa, T. Fujisawa and J. F. Wishart, *J. Phys. Chem. B*, 2010, **114**, 9400-9412.

42. H. Fukazawa, T. Ishida and H. Shirota, *J. Phys. Chem. B*, 2011, **115**, 4621-4631.

43. H. Shirota and T. Ishida, *J. Phys. Chem. B*, 2011, **115**, 10860-10870.

44. F. Bardak, D. Xiao, L. Xue, L. G. Hines, Jr., P. Son, R. A. Bartsch, E. L. Quitevis, P. Yang and G. A. Voth, *ChemPhysChem*, 2012, **13**, 1687-1700.

45. H. Shirota, *ChemPhysChem*, 2012, **13**, 1638-1648.

46. H. Shirota, *J. Phys. Chem. B*, 2013, **117**, 7985-7995.

47. L. Xue, G. Tamas, R. P. Matthews, A. J. Stone, P. A. Hunt, E. L. Quitevis and R. M. Lynden-Bell, *Phys. Chem. Chem. Phys.*, 2015, **17**, 9973-9983.

48. H. Shirota and S. Kakinuma, *J. Phys. Chem. B*, 2015, **119**, 9835-9846.

49. H. Shirota, S. Kakinuma, K. Takahashi, A. Tago, H. Jeong and T. Fujisawa, *Bull. Chem. Soc. Jpn.*, 2016, **89**, 1106-1128.

50. D. McMorrow, *Opt. Commun.*, 1991, **86**, 236-244.

51. D. McMorrow and W. T. Lotshaw, *J. Phys. Chem.*, 1991, **95**, 10395-10406.

52. S. Kinoshita, Y. Kai, M. Yamaguchi and T. Yagi, *Phys. Rev. Lett.*, 1995, **75**, 148-151.

53. R. M. Lynden-Bell and E. L. Quitevis, *Phys. Chem. Chem. Phys.*, 2016, **18**, 16535-16543.

54. J. L. Anderson, R. Ding, A. Ellern and D. W. Armstrong, *J. Am. Chem. Soc.*, 2005, **127**, 593-604.

55. H. Shirota, T. Mandal, H. Fukazawa and T. Kato, *J. Chem. Eng. Data*, 2011, **56**, 2453-2459.

56. A. S. Khan, Z. Man, A. Arvina, M. A. Bustam, A. Nasrullah, Z. Ullah, A. Sarwono and N. Muhammad, *J. Mol. Liquids*, 2017, **227**.

57. E. Bodo, M. Chiricotto and R. Caminiti, *J. Phys. Chem. B*, 2011, **115**, 14341-14347.

58. S. Li, G. Feng, J. L. Banuelos, G. Rother, P. F. Fulvio, S. Dai and P. T. Cummings, *J. Phys. Chem. C*, 2013, **117**, 18251-18257.

59. R. M. Lynden-Bell and E. L. Quitevis, *J. Chem. Phys.*, 2018, **148**, 193844(1)-183844(6).

60. S. V. Dzyuba and R. A. Bartsch, *J. Heterocyclic Chem.*, 2001, **38**, 265-268.

61. S. V. Dzyuba and R. A. Bartsch, *ChemPhysChem*, 2002, **3**, 161-166.

62. E. L. Quitevis and M. Neelakandan, *J. Phys. Chem.*, 1996, **100**, 10005-10014.

63. M. Neelakandan, D. Pant and E. L. Quitevis, *Chem. Phys. Lett.*, 1996, **265**, 283-292.

64. W. T. Lotshaw, D. McMorrow, N. Thantu, J. S. Melinger and R. Kitchenham, *J. Raman Spectrosc.*, 1995, **26**, 571-583.

65. T. Ishida and H. Shirota, *J. Phys. Chem. B*, 2013, **117**, 1136-1150.

66. S. Ryu and R. M. Stratt, *J. Phys. Chem. B*, 2004, **108**, 6782-6795.

67. J. A. Bucaro and T. A. Litovitz, *J. Chem. Phys.*, 1971, **54**, 3846-3853.

68. J. S. Bender, J. T. Fourkas and B. Coasne, *J. Phys. Chem. B*, 2017, **121**, 11376-11382.

69. C. Kalpouzos, D. McMorrow, W. T. Lotshaw and G. A. Kenney-Wallace, *Chem. Phys. Lett.*, 1988, **150**, 138-146.

70. C. Kalpouzos, D. McMorrow, W. T. Lotshaw and G. A. Kenney-Wallace, *Chem. Phys. Lett.*, 1989, **155**, 240-242.

71. D. McMorrow, N. Thantu, J. S. Melinger, S. K. Kim and W. T. Lotshaw, *J. Phys. Chem.*, 1996, **100**, 10389-10399.

72. T. Steffen, N. A. C. M. Meinders and K. Duppen, *J. Phys. Chem. A*, 1998, **102**, 4213-4221.

73. D. McMorrow, N. Thantu, V. Kleinman, J. S. Melinger and W. T. Lotshaw, *J. Phys. Chem. A*, 2001, **105**, 7960-7972.

74. A. Scodinu and J. T. Fourkas, *J. Phys. Chem. B*, 2003, **107**, 44-51.

75. Q. Zhong and J. T. Fourkas, *J. Phys. Chem. B*, 2008, **112**, 15529-15539.

76. E. L. Quitevis, F. Bardak, D. Xiao, L. G. Hines Jr., P. Son, R. A. Bartsch, P. Yang and G. A. Voth, in *Ionic Liquids: Science and Applications*, eds. A. E. Visser, N. J. Bridges and R. D. Rogers, ACS, Washington DC, 2012, vol. 1117, ch. 13, pp. 271-287.

77. T. Keyes, D. Kivelson and J. P. McTague, *J. Chem. Phys.*, 1971, **55**, 4096.

78. T. I. Cox, M. R. Battaglia and P. A. Madden, *Mol. Phys.*, 1979, **38**, 1539-1554.

79. P. A. Madden and D. J. Tildesley, *Mol. Phys.*, 1985, **55**, 969-998.

80. R. M. Lynden-Bell, L. Xue, G. Tamas and E. L. Quitevis, *J. Chem. Phys.*, 2014, **141**, 044506(1)-044506(13).

Table 1. Parameters of the fit of the two-component line-shape function to the CS_2 intermolecular spectra in neat CS_2, 10 mol.% CS_2/MIL(n), and 18.2 mol.% CS_2/DIL(2n) with n = 3-5.[a-d]

System	A_{BL}	a	ω_{BL} / cm^{-1}	f_{BL}	A_{AG}	ω_{AG} / cm^{-1}	ε /cm^{-1}	f_{AG}
Neat	0.143	1.17	19.8	0.75	0.610	46.13	23.5	0.25
MIL(3)	0.052	0.99	14.0	0.49	0.198	32.86	27.9	0.51
MIL(4)	0.039	1.10	12.6	0.43	0.214	32.33	25.9	0.57
MIL(5)	0.031	1.09	14.4	0.46	0.198	31.96	26.1	0.54
DIL(6)	0.003	1.90	7.7	0.26	0.102	36.03	22.3	0.74
DIL(8)	0.008	1.20	14.0	0.19	0.268	35.41	22.2	0.81
DIL(10)	0.003	1.89	10.2	0.34	0.138	35.82	24.4	0.66

[a]From fits of the additivity model (eq 3) to the RSDs. See eqs 6 and 7 for definitions of A_{BL}, a, ω_{BL}, $A_{AG,}$ ω_{AG} and ε.

[b]Fractional areas of component bands - f_{BL}, f_{AG}.

[c]Errors in fit parameters: A_{BL}± 0.001; a ±0.01; ω_{BL} ± 0.6; A_{AG} ± 0.004; ω_{AG} ±0.34; ε ± 0.3.

[d]See Tables S2a-c in ESI for fit parameters for the other CS_2/IL mixtures.

Table 2. CS_2 Intermolecular Spectral Parameters.[a,b]

CS_2 mol %	ω_{pk} / cm^{-1}	$\Delta\omega$ / cm^{-1}	CS_2 mol %	ω_{pk} / cm^{-1}	$\Delta\omega$ / cm^{-1}
	Neat CS_2			Neat CS_2	
100	28	60	100	28	60
	CS_2/MIL(3)			CS_2/DIL(6)	
10	21	52	18.2	27	48
15	24	51	26	25	53
20	20	52	33.3	24	55
25	23	52	40	26	60
	CS_2/MIL(4)			CS_2/DIL(8)	
10	21	50	18.2	30	49
15	24	50	26	28	53
20	19	51	33.3	26	53
25	23	51	40	26	53
	CS_2/MIL(5)			CS_2/DIL(10)	
10	21	52	18.2	27	50
15	24	51	26	25	54
20	19	51	33.3	24	52
25	23	51	40	23	51

[a]Peak frequency -- ω_{pk}; full-width-half-maximum -- $\Delta\omega$.

[b]Error ± 1 cm^{-1}

Table 3. Spectral First Moment M_1 for CS_2 in CS_2/MIL(4) and CS_2/DIL(8) Mixtures.[a]

CS_2/MIL(4)		CS_2/DIL(8)	
CS_2 mol.%	M_1 / cm^{-1}	CS_2 mol.%	M_1 / cm^{-1}
10	35	18.2	40
15	35	26	40
20	35	33.3	37
25	36	40	37
100	44	100	44

[a]See eq 8 for definition of M_1.

Table 4. Calculated Densities and Viscosities of CS_2/MIL(4) and CS_2/DIL(8) Mixtures at 297 K.[a]

CS_2 mol %	ρ / gcm^{-3}	η / mPa-s	CS_2 mol %	ρ / gcm^{-3}	η / mPa-s
	Neat CS_2 (76.13 g mol^{-1})			Neat CS_2 (76.13 g mol^{-1})	
100	1.266	0.354	100	1.266	0.354
	CS_2/MIL(4)			CS_2/DIL(8)	
10	1.434	3.33	18.2	1.493	6.90
15	1.432	2.27	26	1.489	4.84
20	1.429	1.72	33.3	1.485	3.79
25	1.427	1.39	40	1.481	3.16
	Neat MIL(4) (405 g mol^{-1})			Neat DIL(8) (836.7 g mol^{-1})	
0	1.438	49.4	18.2	1.500	662.9

[a]Densities and viscosities of MIL(4) and DIL(8) from ref 19.

[b]Viscosity of CS_2 from CRC Handbook 75th Edition.

[c]Mixture density ρ_{mix} and mixture viscosity η_{mix} calculated using the equations

$$\rho_{mix} = [f_{CS_2} M_{CS_2} + (1 - f_{CS_2}) M_{IL}] / [(f_{CS_2} M_{CS_2} / \rho_{CS_2}) + ((1 - f_{CS_2}) M_{IL} / \rho_{IL})]$$

$$1/\eta_{mix} = f_{CS_2}/\eta_{CS_2} + (1 - f_{CS_2})/\eta_{IL}$$

where M_{CS_2} and M_{CS_2} are the molar masses of CS_2 and the IL, η_{CS_2} and η_{IL} are the viscosities of CS_2 and the IL, ρ_{CS_2} and ρ_{IL} are the densities of CS_2 and the IL, and f_{CS_2} is the mole fraction of CS_2.

Figure Captions

Figure 1. Reduced spectral densities in the 0-400 cm^{-1} range. (Top Row) CS_2/MIL(*n*) with *n* = 3-5, mol.%, top to bottom: 100, 25, 20, 15, 10, 0. (Bottom Row) CS_2/DIL(2*n*) with *n* = 3-5, mol.%, top to bottom: 100, 40, 33.3, 26, 18.2, 0.

Figure 2. Comparison of reduced spectral densities of neat MIL(*n*) (red curves) and neat DIL(2*n*) (blue curves) in the 0-200 cm^{-1} range, normalized at the low-frequency ($\approx$ 20 cm^{-1}) component band.

Figure 3. Reduced spectral density of neat CS_2 (points) in the 0-200 cm^{-1} range. The solid line is a fit of the two-component line-shape function (eq 5) to the RSD with dashed lines being the low-frequency (Bucaro-Litovitz (BL) function, eq 6) and high-frequency (antisymmetrized Gaussian (AG) function, eq 7) components (adapted with permission from ref. 18, copyright 2014. American Institute of Physics). See Table 1 for BL and AG fit parameters.

Figure 4. Representative reduced spectral densities (points) for 10 mol.% CS_2/MIL(*n*) and 18.2 mol.% CS_2/MIL(2*n*) with *n* = 3-5 with the fits of the additivity model (eq 3) and the two-component line-shape function (eq 5) to the RSDs: green curve -- CS_2 contribution; red curve – IL contribution. The dashed lines are the low-frequency (Bucaro-Litovitz function, eq 5) and high-frequency (antisymmetrized Gaussian function, eq 6) components. See Table 1 for two-component line-function fit parameters. See Figures S2a-c and S3a-c for RSDs and fits of the model to the RSDs of other CS_2/IL mixtures and Tables S2a-c for corresponding BL and AG fit parameters.

Figure 5. Height-normalized CS_2 contributions (solid lines) to the reduced spectral densities of CS_2/MIL(n) with n = 3-5 mixtures (top row). Height-normalized CS_2 contributions (solid lines) to the reduced spectral densities of CS_2/DIL(2n) with n = 3-5 mixtures (bottom row). RSD of neat CS_2 (dash line) shown for comparison in each plot. See Table 2 for values of the peak frequency ω_{pk} and full-width-at-half-maximum $\Delta\omega$.

Figure 6. Plots of the values of the peak frequency, ω_{pk}, of the CS_2 contributions to RSDs of CS_2/MIL(n) with n = 3-5 mixtures and RSDs of CS_2/DIL(2n) mixtures with n = 3-5 versus CS_2-to-Ring mol % which is equal to the CS_2/MIL(n) mol.%. See Table 2 for values of ω_{pk}.

Figure 7. Comparison of CS_2 contributions to the reduced spectral densities of the 10 mol.% CS_2/MIL(4) and 18.2 mol% CS_2/DIL(8) mixtures (left). Comparison of simulated librational densities of states for CS_2 in 10 mol % CS_2/MIL(4) and 18.2 mol % CS_2/DIL(8) (right) (adapted with permission from ref. 59, copyright 2018. American Institute of Physics).

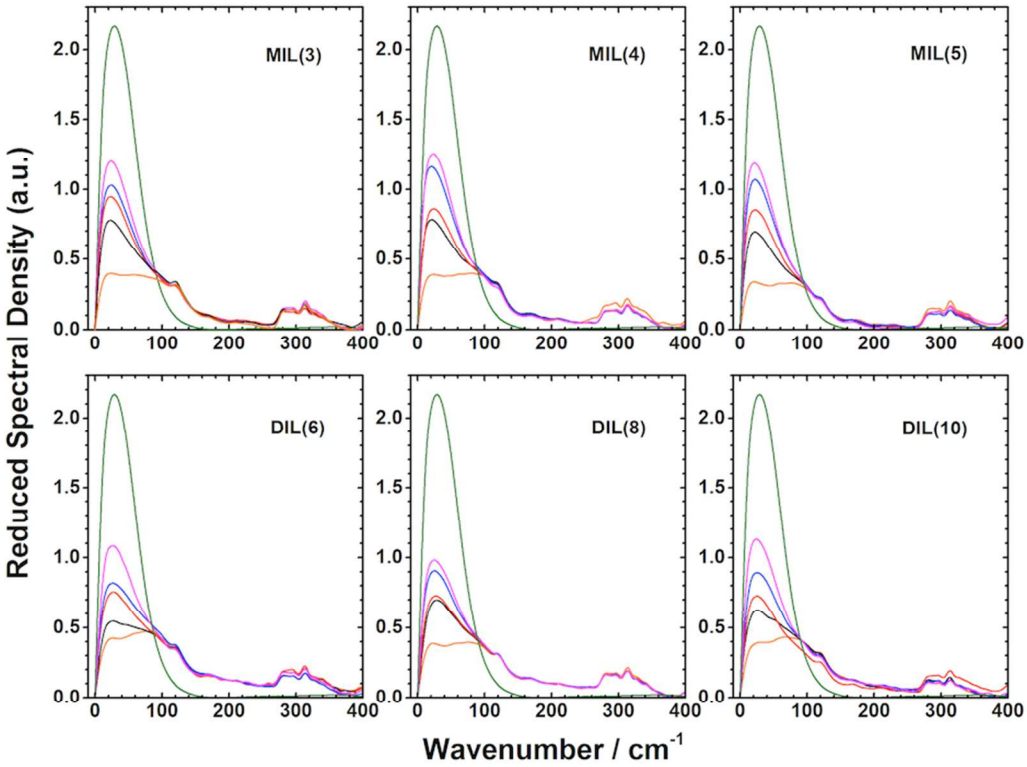
MIL(3)
MIL(4)
MIL(5)
DIL(6)
DIL(8)
DIL(10)
Reduced Spectral Density (a.u.)
Wavenumber / cm-1
0.0
0.5
1.0
1.5
2.0
0
100
200
300
400

Figure 1

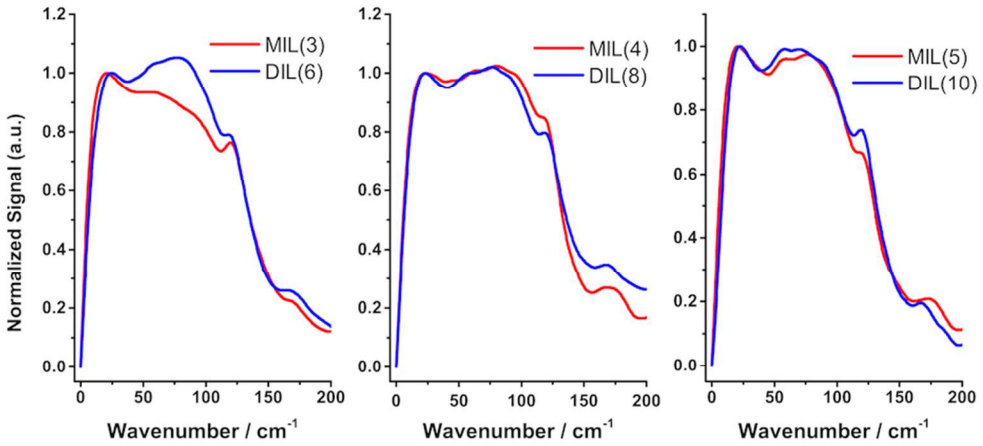
Normalized Signal (a.u.)
MIL(3)
DIL(6)
MIL(4)
DIL(8)
MIL(5)
DIL(10)
Wavenumber / cm-1
Wavenumber / cm-1
Wavenumber / cm-1

Figure 2

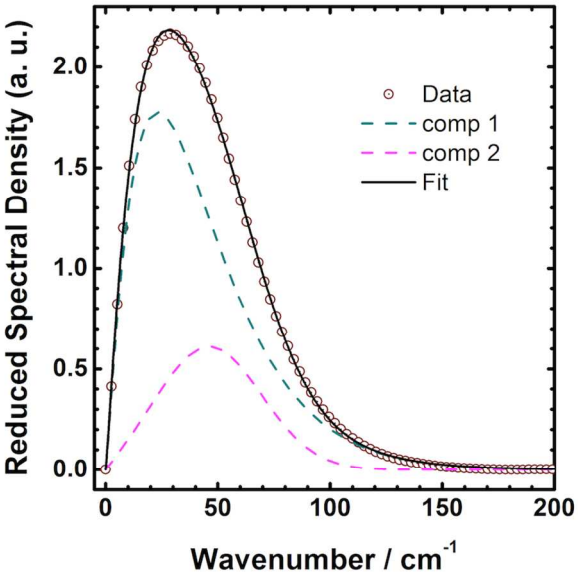
Reduced Spectral Density (a. u.)
2.0
1.5
1.0
0.5
0.0
0
50
100
150
200
Wavenumber / cm-1
Data
comp 1
comp 2
Fit

Figure 3

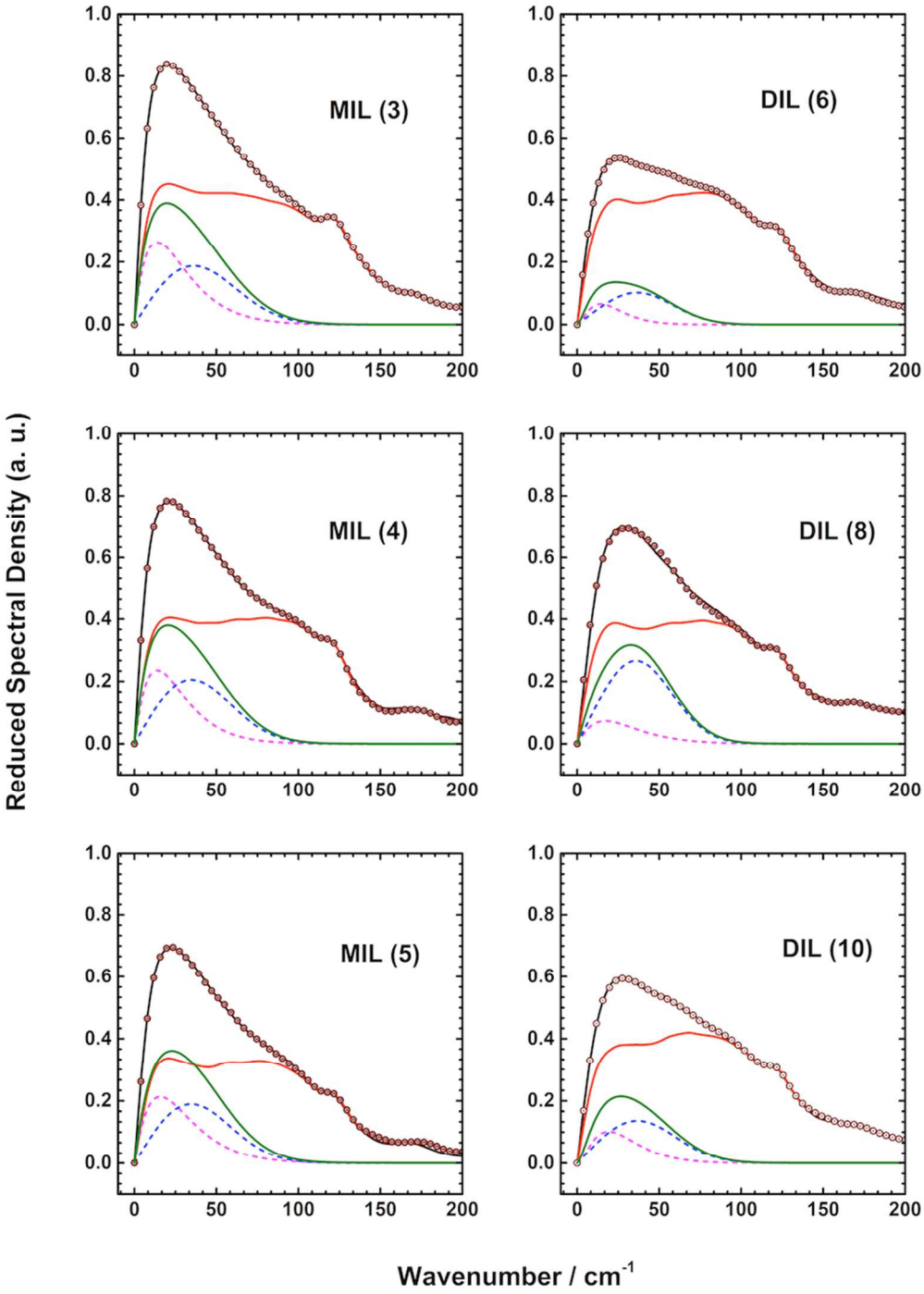
MIL (3)
DIL (6)
MIL (4)
DIL (8)
MIL (5)
DIL (10)
Reduced Spectral Density (a. u.)
Wavenumber / cm-1
0.0
0.2
0.4
0.6
0.8
1.0
0
50
100
150
200

Figure 4

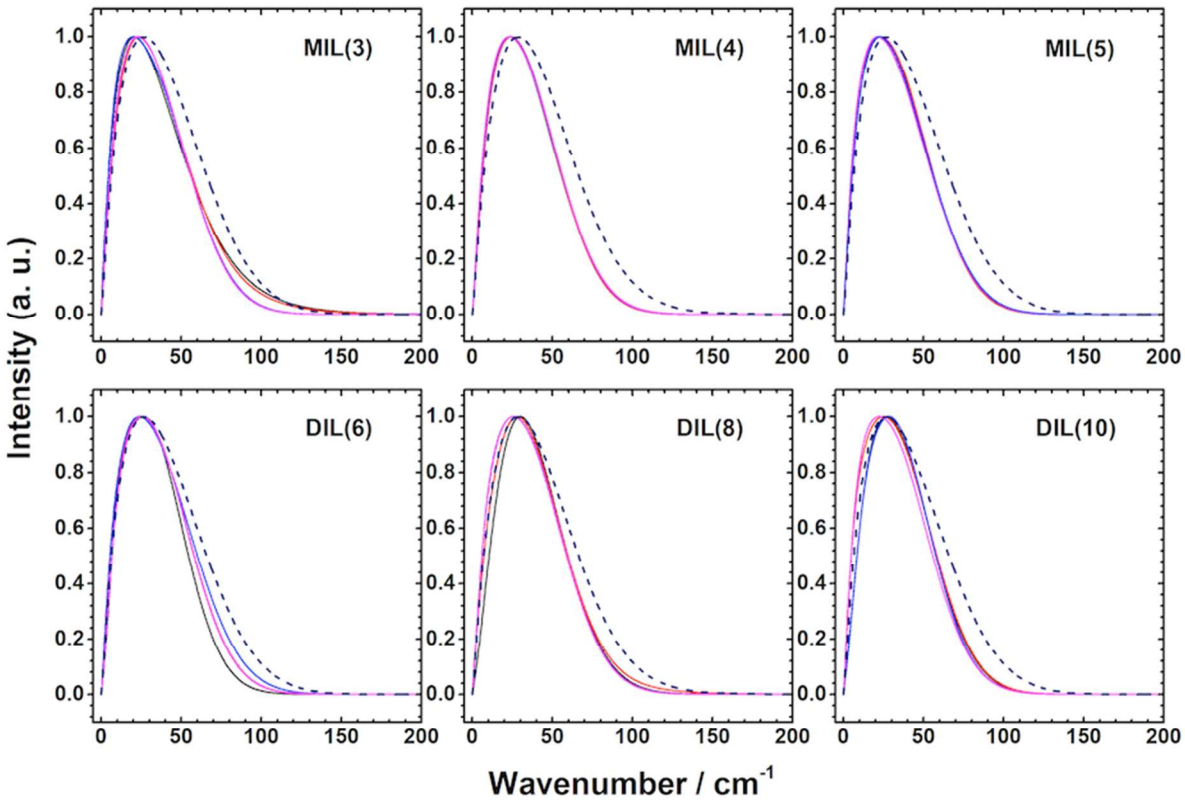
MIL(3)
MIL(4)
MIL(5)
DIL(6)
DIL(8)
DIL(10)
Intensity (a. u.)
Wavenumber / cm-1
0.0
0.2
0.4
0.6
0.8
1.0
0
50
100
150
200

Figure 5

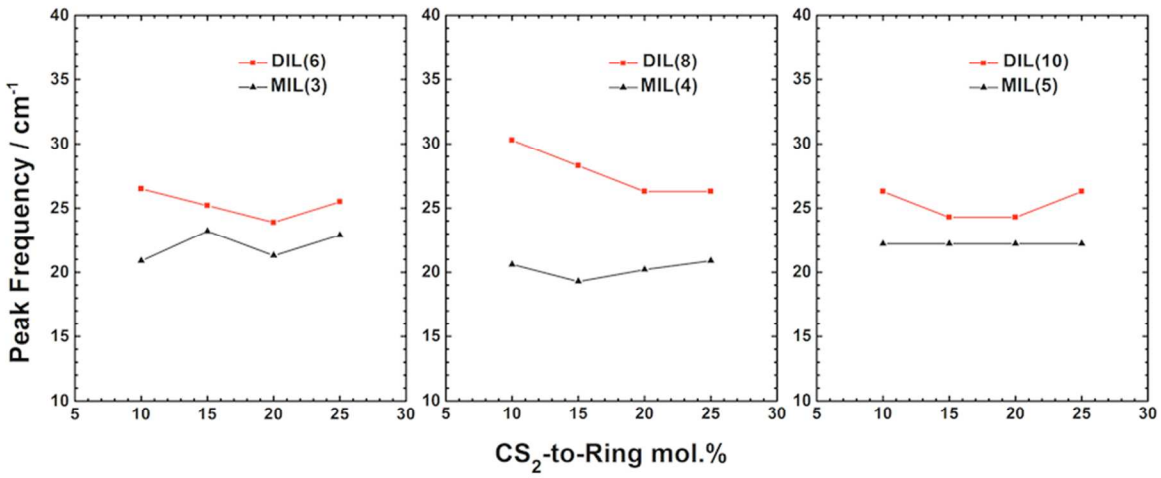
DIL(6)
MIL(3)
DIL(8)
MIL(4)
DIL(10)
MIL(5)
Peak Frequency / cm-1
CS2-to-Ring mol.%

Figure 6

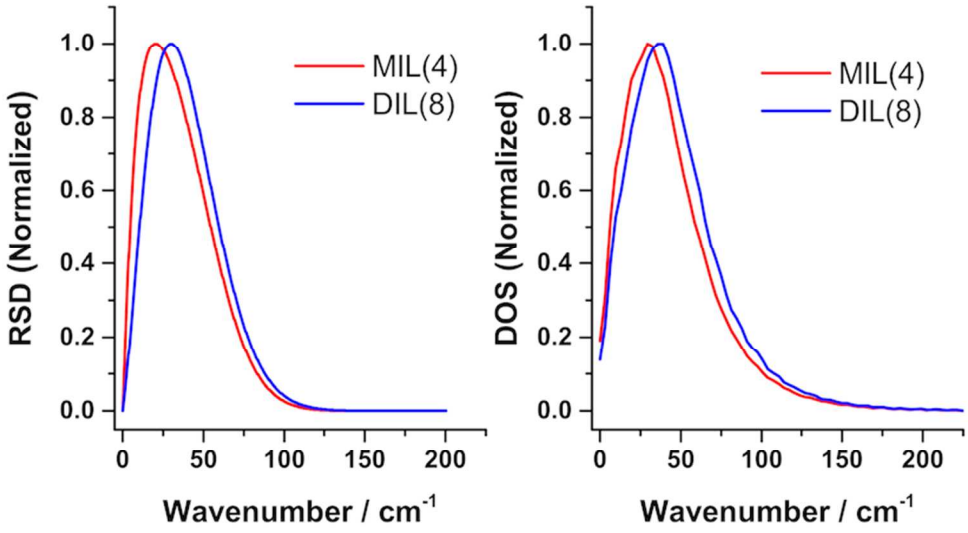
RSD (Normalized)
1.0
0.8
0.6
0.4
0.2
0.0
0
50
100
150
200
Wavenumber / cm-1
MIL(4)
DIL(8)
DOS (Normalized)
1.0
0.8
0.6
0.4
0.2
0.0
0
50
100
150
200
Wavenumber / cm-1
MIL(4)
DIL(8)

Figure 7

Graphical Abstract:

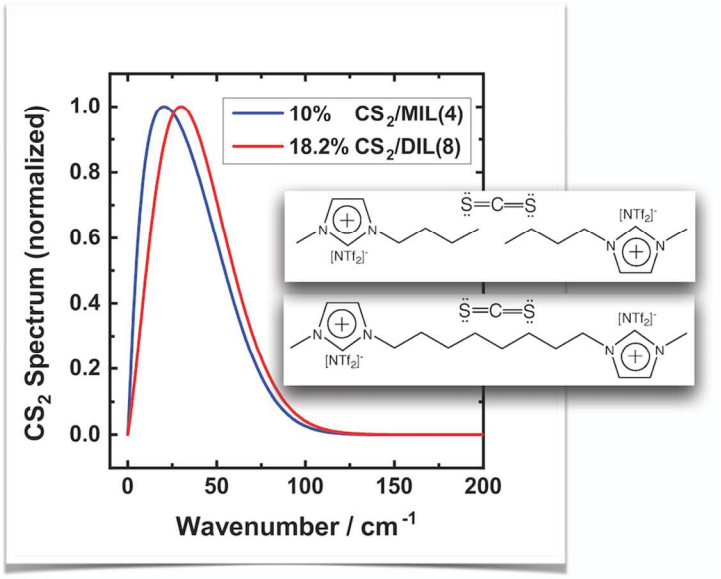

The intermolecular dynamics of CS_2 are higher in frequency in dicationic than in monocationic IL solution because of confinement effects.